Memoirs of the Faculty of Engineering, Okayama University, Vol.35, Nos.1&2, pp.53-61, March 2001

Focusing Characteristic Analysis of Circular Fresnel Zone Plate Lens

Tae Yong KIM[1] and Yukio KAGAWA[2]

(Received December 19, 2000)

Fresnel zone plate lens (FZPL) has widely been used in electromagnetic antenna applications. Most analysis method based on the potential (scalar) wave approximation has been applied to a few very limited and simplified cases. The present paper analyzes the FZPL in more general form including the diffraction and transmission using the method of moments (MoM). The focusing gain characteristics in the oblique incidence as well as in the normal incidence are considered. The MoM solution using the three-dimensional vectorial formulation requires a large memory space for the FZPL as it is operated at a short wavelength. This is simply overcome by using an iterative conjugate gradient method for the numerical evaluation. The MoM solutions are compared with the other solutions.

1 INTRODUCTION

Fresnel zone plate lenses have been used as a flat optical lens [1]. Their equivalence has also widely been used in electromagnetic antenna applications. The use for receiver antennas of the communication satellite televisions, radio astronomical observation and so on, is reported because of their structural simplicity and low cost [2]. Hoashi et al. reported the evaluation of a FZPL antenna based on Kirchhoff's scalar formula [3]-[4]. Guo et al. considered the far-field analysis for the offset FZPL antenna design [5].

In the present paper, the FZPL is considered as the electromagnetic scattering and diffraction problems in the exact manner, for which numerical techniques are attempted to solve the fundamental field equations, subject to the boundary conditions and the geometry constraints. The formulation is presented and the MoM is applied as a solution method. The MoM is a direct boundary integral equation method, suitable for the analysis of electromagnetic scattering and diffraction problems [6]-[10]. The MoM reduces the integral equation to a set of linear algebraic equation. Although the application is direct, however, when the dimension of the object is large relative to the wavelength to be considered, enormous computational resources are required. This is simply overcome by using a restart conjugate gradient method for the numerical solutions [8]-[10]. Some numerical simulation results and the comparison with other solutions are presented.

2 MOMENT METHOD FORMULATION

The operation of the zone plate lens antenna is based on the wave interference as the results the diffraction, scattering and the radiation from the induced surface currents. The integral expression is applied to 3-D surface

[1]The Graduate School of Natural Science and Technology
[2]Department of Electrical and Electronic Engineering

of the conducting bodies of arbitrary shape for the electric field. The boundary condition is enforced in such a way that the tangential electric field vanishes on the perfectly conducting surface

$$\boldsymbol{n} \times \boldsymbol{E}^{inc} = \boldsymbol{n} \times (j\omega \boldsymbol{A}) + \boldsymbol{n} \times \nabla \Phi \quad \text{on } S \tag{1}$$

where $\boldsymbol{n}$ denotes the outward unit normal vector on the conducting surface S, $\boldsymbol{E}^{inc}$ is an impressed electric field and ω denotes the angular frequency. The magnetic vector potential $\boldsymbol{A}$ and the electric scalar potential Φ are derived as the following:

$$\boldsymbol{A}(\boldsymbol{r}) = \mu \int_{S'} \boldsymbol{J}(\boldsymbol{r}') G(\boldsymbol{r}, \boldsymbol{r}') dS' \tag{2}$$

$$\Phi(\boldsymbol{r}) = \frac{j}{\omega \varepsilon} \int_{S'} (\nabla' \cdot \boldsymbol{J}(\boldsymbol{r}')) G(\boldsymbol{r}, \boldsymbol{r}') dS' \tag{3}$$

$$G(\boldsymbol{r}, \boldsymbol{r}') = \frac{e^{-jkR}}{4\pi R} \tag{4}$$

where $k = \omega(\varepsilon\mu)^{1/2}$ represents the wave number corresponding to the external medium (permittivity ε, permeability μ) and $R = |\boldsymbol{r} - \boldsymbol{r}'|$. $\boldsymbol{r}$ and $\boldsymbol{r}'$ are the position vectors at a field point and at the source point, respectively.

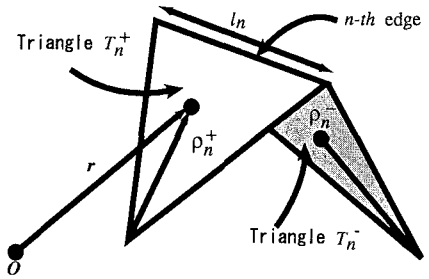

Figure 1 Triangular surface elements sharing a common edge l_n.

The unknown current distributions $\boldsymbol{J}(\boldsymbol{r}')$ is expanded to be solved in the form:

$$\boldsymbol{J} \simeq \sum_{n=1}^{N} J_n \boldsymbol{f}_n \tag{5}$$

where J_n is the unknown current coefficient and $\boldsymbol{f}_n$ is the known expansion function. As shown in Figure 1, the expansion function $\boldsymbol{f}_n$ is definded on a pair of triangular patches T_n^+ and T_n^- sharing a common edge l_n as:

$$\boldsymbol{f}_n = \frac{l_n}{2A_n^{\pm}} \boldsymbol{\rho}_n^{\pm} \quad \text{for } T_n^{\pm} \tag{6}$$

where l_n is the length of the common edge, $A_n^{\pm}$ is the area of the triangle patch $T_n^{\pm}$, and $\boldsymbol{\rho}_n^{\pm}$ is the position vector with respect to $T_n^{\pm}$ [6]. Both sides of Equation (1) are integrated over the surface S, so that the MoM expression is:

$$< \boldsymbol{f}_m, \boldsymbol{E}^{inc} > = j\omega < \boldsymbol{f}_m, \boldsymbol{A} > + < \boldsymbol{f}_m, \nabla \Phi > \tag{7}$$

where the notation $< \boldsymbol{a}, \boldsymbol{b} >$ denotes a symmetric inner product or $\int_S \boldsymbol{a} \cdot \boldsymbol{b} dS$. Here the weighting function $\boldsymbol{f}_m$ is chosen to be the same as the expansion function $\boldsymbol{f}_n$. The linear algebraic equation is thus obtained

$$\begin{aligned} \sum_{n=1}^{N} Z_{mn} J_n &= V_m \\ \text{or} \quad [Z_{mn}]\{J_n\} &= \{V_m\}, \quad m = 1, 2, \cdots, N \end{aligned} \tag{8}$$

where Z_{mn} is a generalized system matrix and V_m is a driving vector depended on an excitation. This fully occupied equation system has to be solved numerically for the unknown current coefficient J_n. Especially for a large-scale electromagnetic problems, the system matrix Z_{mn} is large, full and dense. The iterative conjugate gradient method is applied to solve the discretized linear system for the numerical solution.

3 DETERMINATION OF A FRESNEL ZONE CONFIGURATION

A typical FZPL consists of the closed conductive opaque annuli rings as shown in Figure 2. The conducting opaque zones are assumed to lie in the x-y plane, centered at $(0,0,0)$ in the Cartesian coordinates. The focal point must lie at $(0,0,F)$, where F is the focal length. According to the concept of the Fresnel's principle, the focal point is created in such a way that rays via the boundaries of the rings yield successively path-length difference of one-half of the wavelength. The relation of the inner and outer radius of j-th zone in the FZPL is thus determined based on the optical ray theory as:

$$R_j^{out} = \sqrt{(F + j\lambda_0 + \lambda_0/4)^2 - F^2} \tag{9}$$

$$R_j^{in} = \sqrt{(F + (j-1/2)\lambda_0 + \lambda_0/4)^2 - F^2} \tag{10}$$

where λ_0 is the wavelength corresponding to the operation frequency in free space [4]. As shown in Figure 3, the two complementary formulations are possible for diffraction with conductive rings and transmission through the apertures. Kirchhoff scalar wave approximation can be applied to solve the transmission through the aperture.

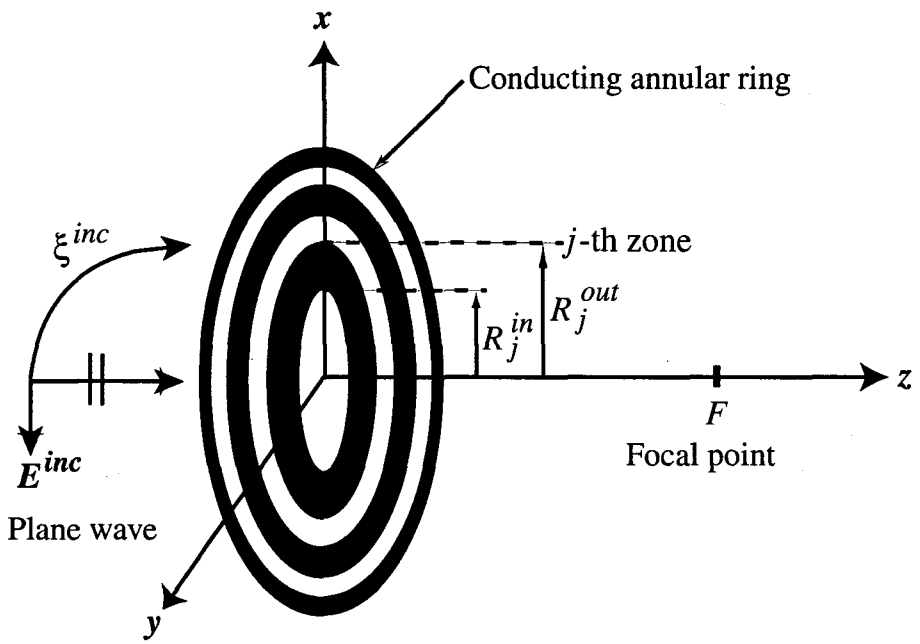

Figure 2 Geometry of a circular Fresnel zone-plate lens.

4 NUMERICAL RESULTS

In this section, the numerical results are presented for some example of Fresnel zone plate lenses. The geometry for the FZPL is determined based on Equation (9) and (10). The conducting annuli rings are discretized to triangular patches. Since the unknown coefficients of the induced current are obtained by solving the system of equations. The scattered electric field can be calculated directly from the induced currents. The scattered near field solution from the conducting zone plates can also be obtained from the physical optics (PO) [11], which

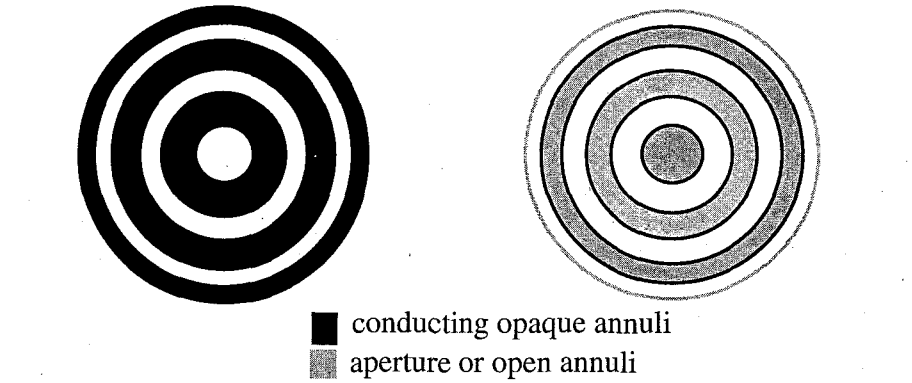

Figure 3 Two complementary models for the FZPL.

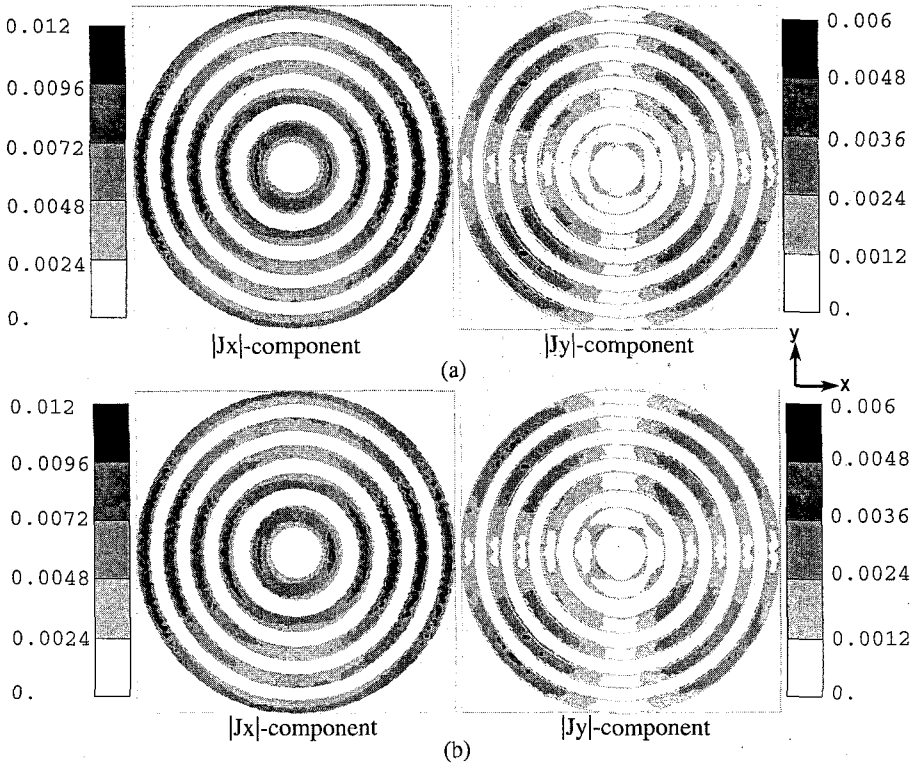

Figure 4 Computed surface current distributions(F=5 cm, λ_0=2.5 cm): (a) is the magnitude patterns for the case $\xi^{inc} = 0^o$ and (b) is the magnitude patterns for the case $\xi^{inc} = 4^o$.

is, to be exact, limited to an electrically large scatterer. For the complementary solution method, traditional Kirchhoff's approximation can be applied on a short wavelength wave such as the aperture problem, as shown in Figure 3(b).

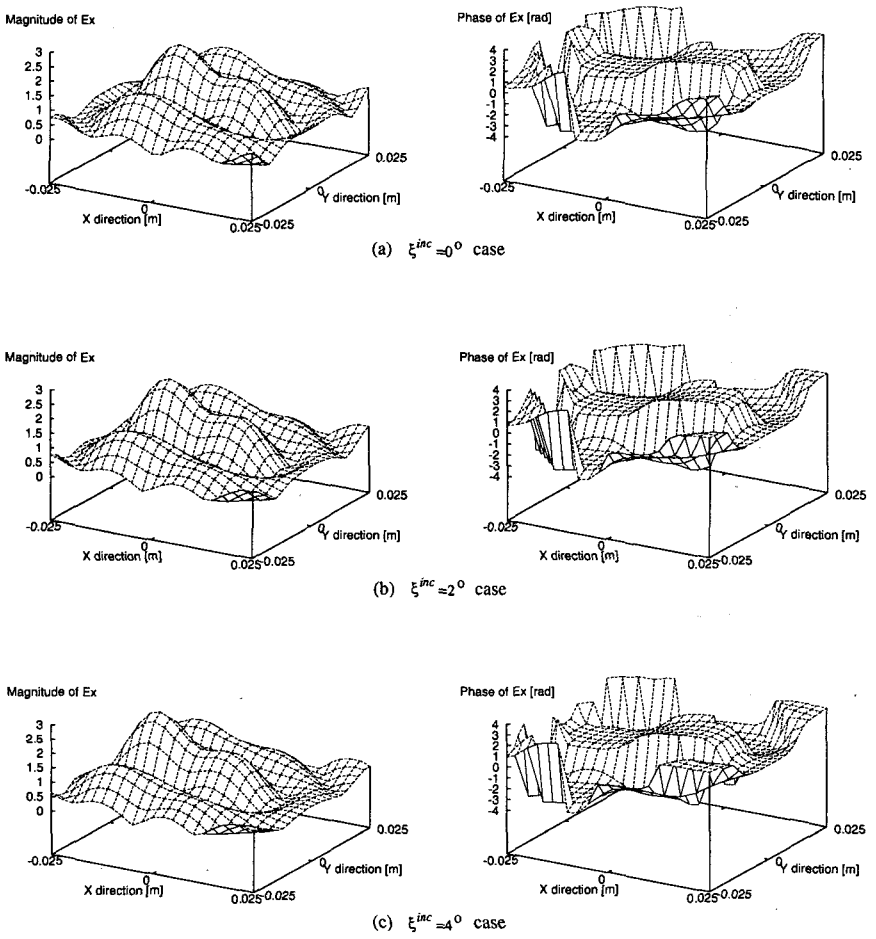

Figure 5 Electric field distributions of the dominant component for various incident angles in z=5 cm plane (F=5 cm, λ_0=2.5 cm).

The FZPL for the five conducting opaque rings is considered and operated at 11.92GHz ($\lambda_0 = 2.5$ cm). The focal length is supposed to be $F = 5.0$ cm ($=2\lambda_0$). Assume that x-polarized plane wave with incident angle ξ^{inc} arrives from the left side of the FZPL as shown in Figure 2. The conductive zone rings are divided into 5352 triangular elements with 7224 unknowns.

Figure 4 shows the magnitude patterns for the computed surface current distributions of each component for various incident angles. Note that y-component as well as x-component for the induced currents on conducting annuli rings also exists. In fact, if the aperture size is large in terms of the wavelength, the aperture field may be approximately equal to those of the incident field except the field near the edges for Kirchhoff's approximation. In the PO method, the surface currents are also considered to be the incident electric field so that y-component of the induced surface currents is not exist. Consequently, the solutions computed from the PO method and Kirchhoff's approximation are not included these y-component surface current for the next axial focal characteristic calculations. The electric field distributions of a dominant component in the receiving plane, z=5 cm plane ($X-Y$ plane), for the various incident angle are shown in Figure 5. Although the incident angle is obliquely various, the patterns of the field distributions in the receiving plane are fixed.

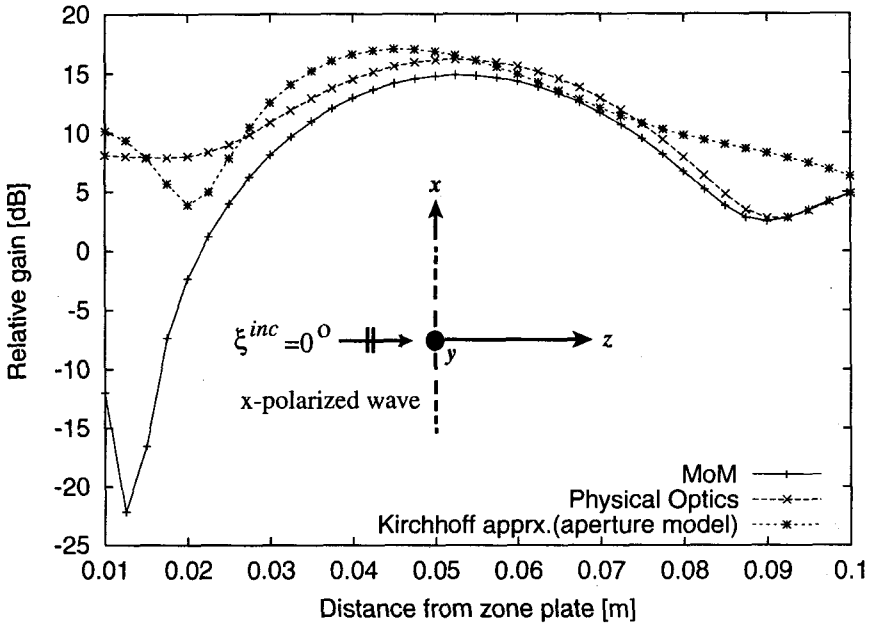

Figure 6 Relative field intensity distributions (in decibels) along the axis from the FZPL (F=5 cm, λ_0=2.5 cm, $\xi^{inc} = 0^o$).

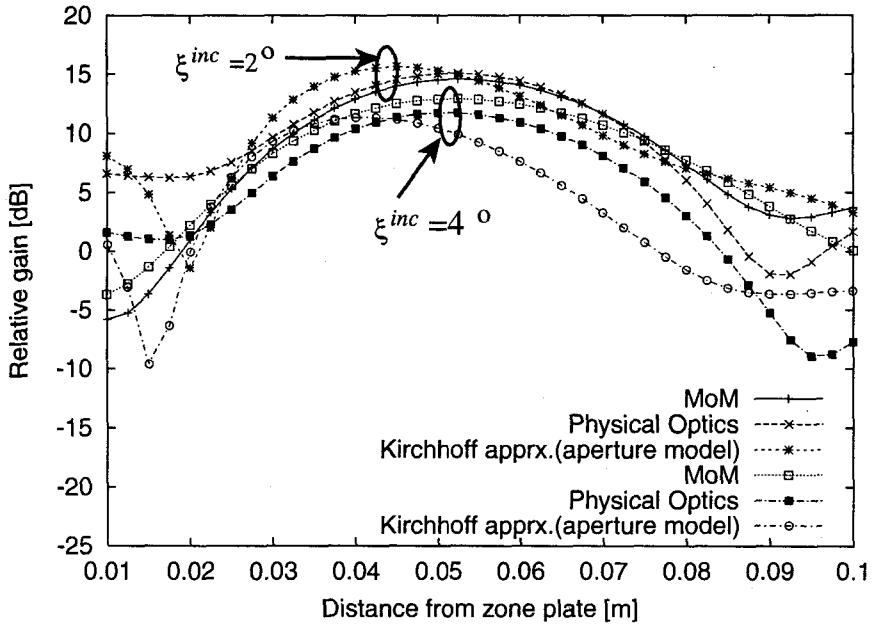

Figure 7 Relative field intensity distributions (in decibels) along the axis from the FZPL for oblique incident case (F=5 cm, λ_0=2.5 cm).

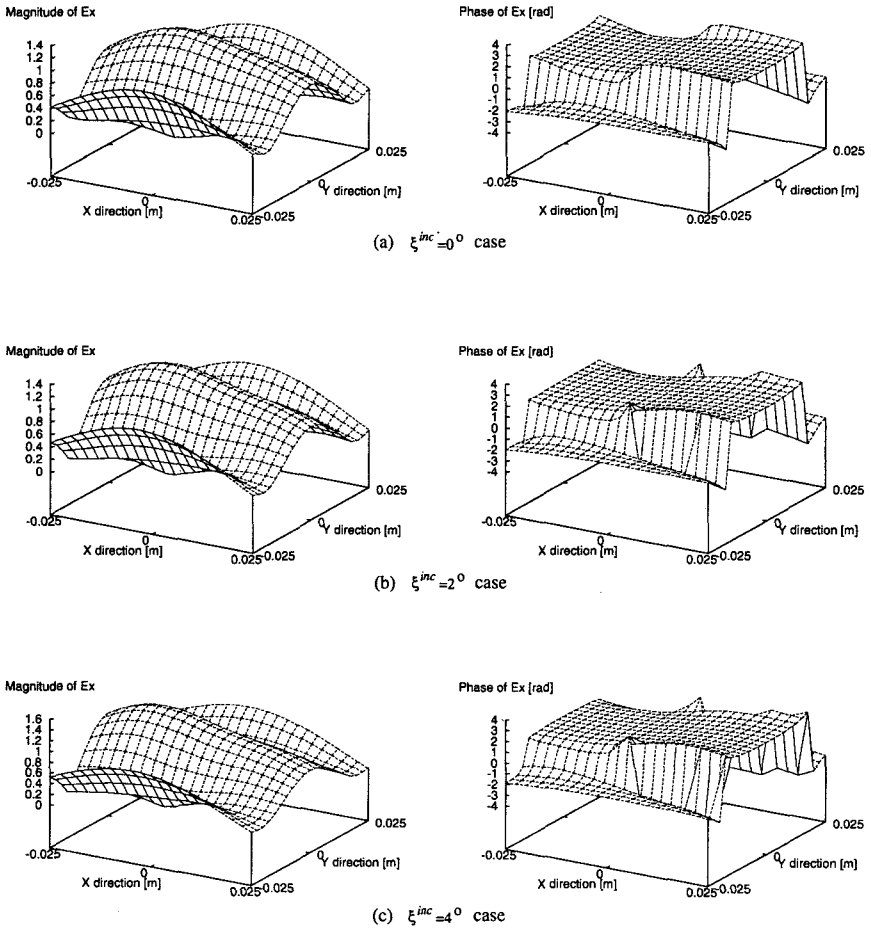

Figure 8 Electric field distributions of the dominant component for various incident angles in z=30 cm plane (F=30 cm, λ_0=2.5 cm)

Figure 6 shows the field intensity distributions along the axis for the plane wave of the normal incidence ($\xi^{inc} = 0^o$). The plus signed line refers to the solutions due to the MoM, which is compared with other solution methods, PO method and Kirchhoff's scalar wave approximation. The discrepancy for the magnitude of each solution is happened. It is occurred that y-component of the induced currents is ignored in the solutions of the PO method and Kirchhoff's approximation. The location of the focal point or the point of the maximum gain is slightly shorter for the solution with Kirchhoff approximation than F=5.0 cm. The field intensity distributions for oblique incidence are then investigated which is shown in Figure 7.

Next, the examination is extended to the case of a longer focal length. The FZPL is designed for three-zone lens and F=30 cm ($12\lambda_0$) at the same operation frequency. The rings are divided into 11080 triangle elements with 15876 unknowns. The electric field distributions of a dominant component in z=30 cm plane ($X-Y$ plane) for the various incident angle are depicted in Figure 8.

The calculated gains versus the distance from the zone plate lens are shown in Figure 9 for the normal incidence. The focusing characteristics for the oblique incidence are shown in Figure 10. The PO method gives closer solutions to the MoM. In some cases and in some regions, Kirchhoff approximation is not too bad. For incident angle $\xi^{inc} = 4^o$, the focal point may not lie on the axis so that the magnitude of the solutions is decreased.

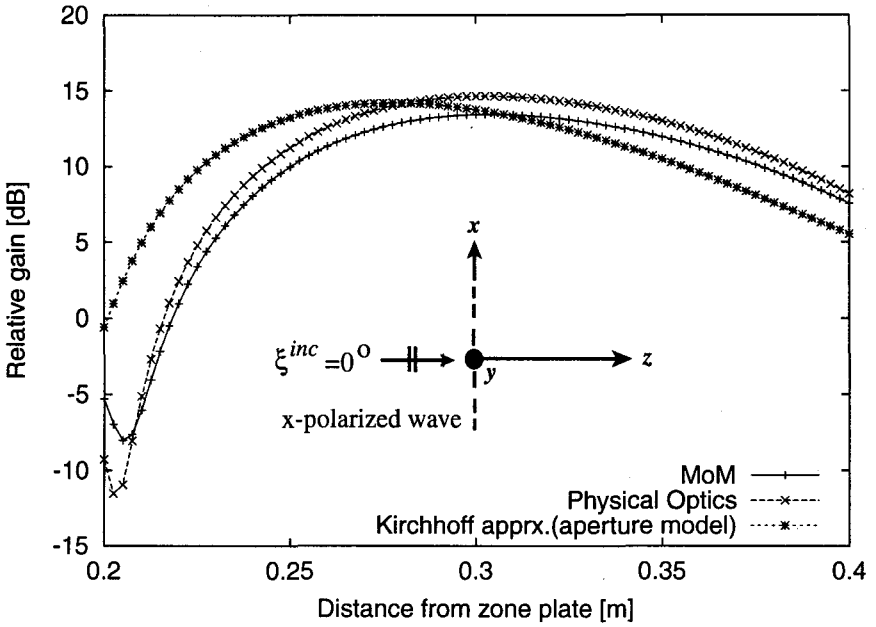

Figure 9 Relative field intensity distributions (in decibels) along the axis from the FZPL (F=30 cm, λ_0=2.5 cm, $\xi^{inc} = 0^o$).

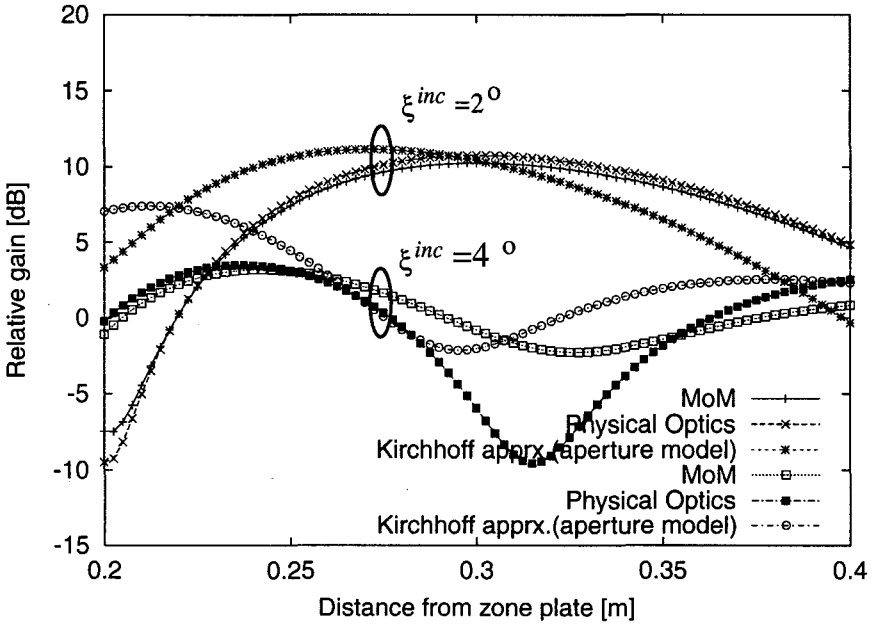

Figure 10 Relative field intensity distributions (in decibels) along the axis from the FZPL for oblique incident case(F=30 cm, λ_0=2.5 cm).

5 CONCLUSIONS

The MoM technique is very general and applicable to the variety of problems. The FZPL is considered as an electromagnetic scattering and diffraction model to which the MoM is applied. The FZPL is operated at a relatively short wavelength. The MoM solution leads to a large system matrix, which could be handled by the iterative conjugate gradient method of a restart version for the numerical solutions. Numerical results have been presented including the oblique incidence, which are compared with other solutions.

References

1. F.A. Jenkins and H.E. White, *Fundamentals of optics*, McGraw-hill Book Company, 1981.

2. Hristo D. Hristov, *Fresnel Zones in wireless links, zone plate lenses and antennas*, Artech House Publishers, 2000.

3. T. Hoashi, T. Onodera and Y. Kagawa, Oblique incidence characteristics of Fresnel-zone plate lens antenna, *Trans. EIC Japan* **J-81-B-II**(8), pp. 823-828, 1998.

4. T. Hoashi, T. Onodera, F. Hagio and Y. Kagawa, On the evaluation of receiving power of a Fresnel-zone-plate lens antenna, *Trans. EIC Japan* **J-79-B-II**(11), pp. 959-963, 1996.

5. Y. J. Guo and S. K. Barton, Offset Fresnel zone plate antenna, *Internation J. Satellite Communication* **12**, pp. 381-384, 1994.

6. S. M. Rao, D. R. Wilton and A. W. Glisson, Electromagnetic scattering by the surfaces of srbitrary shape, *IEEE Trans.* **AP-30**, pp. 409-418, 1982.

7. T. Y. Kim and Y. Kagawa, Electromagnetic scattering from inhomogeneous material bodies, *JASCOME* **Vol. 14**, pp. 19-24, 1997.

8. T. Y. Kim, Y. Kagawa and T. Hoashi, Electromagnetic wave scattering and diffraction from arbitrarily shaped structures, *KJJC-AP/EMC/EMT'98*, pp. 49-52, 1998.

9. Peter M. VAN DEN BERG, Iterative computational techniques in scattering based upon the integrated square error criterion, *IEEE Trans.* **AP-32**, pp. 1063-1071, 1984.

10. Johnson J.H. Wang and John R. Dubberley, Computational of fields in an arbitrarily shaped heterogeneous dielectric ot biological body by an iterative conjugate gradient method, *IEEE Trans.* **MTT-37**, pp. 1119-1125, 1989.

11. Asoke K. Bhattacharyya, *High-frequency electromagnetic techniques*, John Wiley & Sons, 1995.